Supplementary Information:

Thresholds for post-rebound viral control after CCR5 gene-edited autologous hematopoietic cell transplantation

E. Fabian Cardozo[1], Elizabeth R. Duke[1,3], Christopher W. Peterson[2,3], Daniel B. Reeves[1], Bryan T Mayer[1], Hans-Peter Kiem[2,3,4], Joshua T. Schiffer[1,2,3,*]

Description

In this supplementary information we include additional details for model fitting as well as supplementary figures, tables, and references.

Contents

1 Notes on the statistical model

To model the longitudinal T cell and viral load observations for all animals we used a nonlinear, mixed-effects modeling approach. Within this approach we modeled a state variable vector v with observations at time i for each animal j as,

$$v_{ij} = f_v\left(t_{ij}, \Psi_j\right) + \epsilon_v, \tag{S1}$$

where f_v is a nonlinear function for the state variable vector v at an individual observation time, t_{ij}, with animal-specific parameter Ψ_j. The distribution of measurement noise, ϵ_v, is normally distributed with a state-variable-specific standard deviation σ_v,

$$\epsilon_v \sim \mathcal{N}\left(0, \sigma_v^2\right). \tag{S2}$$

Finally, we used a mixed-effects model for each estimated parameter. We assumed that for an animal j each single parameter $\psi_j \in \Psi_j$ is drawn from a probability distribution across the population. This distribution includes the fixed effects $\bar{\psi}$ representing the median value over the the population, and the random effects η_j representing its variability in the population, assumed to be normally distributed with standard deviation σ_ψ, that is

$$\eta_j \sim \mathcal{N}\left(0, \sigma_\psi^2\right). \tag{S3}$$

The non-linear function, f_v, for the given state variables are estimated using numerical solutions of the differential equations models described in more detail below. We fit each model to all data points from all animals simultaneously using a maximum likelihood approach. We assumed that individual observations of each state variable v_{ij} for each animal j at each time point t_i are independent. For each model we estimated the standard deviation of the measurement error for the observations σ_v, and each parameter fixed effects $\bar{\psi}$ and standard deviation of the random effects σ_ψ using the Stochastic Approximation of the Expectation Maximization (SAEM) algorithm embedded in the Monolix software (www.lixoft.eu)[1].

2 Notes on fitting T cell reconstitution before ATI

2.1 Mathematical modeling

We first fit the observed blood T cell kinetics after hematopoetic stem and progenitor cell (HSPC) transplantation and before analytical treatment interruption (ATI). During this procedure, we defined the vector for the state variables $v^{(1)}$ as

$$v^{(1)} = \{S, N, C, M, E\}, \tag{S4}$$

representing the observed blood CD4$^+$CCR5$^-$, CD4$^+$CCR5$^+$, total CD8$^+$, CD8$^+$ T_N + T_{CM}, and CD8$^+$ T_{EM} cell counts, respectively.

We modeled the kinetics of $v^{(1)}$ using a nonlinear ordinary differential equation (ODE) system with solution $f_v^{(1)}$. This ODE model is based on the following assumptions. Transplanted HSPCs, represented by variable T, home to the bone-marrow at a rate k_e. A single cell compartment exists for T cell progenitors in the bone marrow (BM)/thymus. Represented by variable P, these cells renew logistically with maximum rate r_p, differentiate into naive CD4$^+$ and CD8$^+$ T cells at rates λ_f and λ_e, respectively, or are cleared at rate d_p. We modeled two CD4$^+$ T cell compartments: SHIV-non-susceptible, N (CD4$^+$ CCR5$^-$ cells), and SHIV-susceptible, S (CD4$^+$CCR5$^+$ cells). Only the N compartment includes CD4$^+$ naive cells coming from the thymus at an input rate $\lambda_f P$ cells per day. N cells grow with maximum rate r_n, upregulate CCR5 at rate λ_n, and are cleared from the periphery at rate d_n. The S compartment does not have a thymic input but can grow with maximum division rate r_s, downregulate CCR5 at a rate λ_s, and are cleared at rate d_s. We modeled CD8$^+$ T cell reconstitution assuming a compartment for naïve and central memory cells, M, and a compartment for the effector memory subset, E. We assumed that M cells have thymic input of $\lambda_e P$ cells per day, grow logistically with maximum division rate r_m, differentiate to effector memory at rate λ_m , and are cleared at rate d_m. The E compartment grows with maximum division rate r_e and is cleared at rate d_e. CD4$^+$ and CD8$^+$ T cells compete for resources as governed by a logistic equation that depends on the ratio of the total number of T cells, i.e. $N + S + M + E$, to a carrying capacity K. Under this assumptions the model form is:

$$
\begin{aligned}
\frac{dT}{dt} &= -k_e T \\
\frac{dP}{dt} &= k_e T + r_p \left(1 - \frac{N+S+M+E}{K_p}\right) P - d_p P - (\lambda_f + \lambda_e) P \\
\frac{dN}{dt} &= \lambda_f P + \lambda_s S + r_n \left(1 - \frac{N+S+M+E}{K_n}\right) N - \lambda_n N - d_n N \\
\frac{dS}{dt} &= \lambda_n N + r_s \left(1 - \frac{N+S+M+E}{K_s}\right) S - \lambda_s S - d_s S \\
\frac{dM}{dt} &= \lambda_e P + r_m \left(1 - \frac{N+S+M+E}{K_m}\right) M - \lambda_m M - d_m M \\
\frac{dE}{dt} &= \lambda_m M + r_e \left(1 - \frac{N+S+M+E}{K_e}\right) E - d_e E.
\end{aligned}
\tag{S5}
$$

In this model we assumed that the total number of CD8$^+$ T cells is defined as $C = M + E$.

2.2 Model fitting

We first adapted the mechanistic model in **equation S5** using the following substitutions: $\hat{r}_p = r_p - (\lambda_f + \lambda_e + d_p)$, $\hat{r}_n = r_n - (\lambda_n + d_n)$, $\hat{r}_s = r_s - (\lambda_s + d_s)$, $\hat{r}_m = r_m - (\lambda_m + d_m)$, $\hat{r}_e = r_e - d_e$, as well as $K_w = K\frac{\hat{r}_w}{r_w}$ for each model variable $w \in [p, n, s, m, e]$. Using these definitions, the model we used for fitting had the form:

$$
\begin{aligned}
\frac{dT}{dt} &= -k_e T \\
\frac{dP}{dt} &= k_e T + \hat{r}_p \left(1 - \frac{N+S+M+E}{K_p}\right) P \\
\frac{dN}{dt} &= \lambda_f P + \lambda_s S + \hat{r}_n \left(1 - \frac{N+S+M+E}{K_n}\right) N \\
\frac{dS}{dt} &= \lambda_n N + \hat{r}_s \left(1 - \frac{N+S+M+E}{K_s}\right) S \\
\frac{dM}{dt} &= \lambda_e P + \hat{r}_m \left(1 - \frac{N+S+M+E}{K_m}\right) M \\
\frac{dE}{dt} &= \lambda_m M + \hat{r}_e \left(1 - \frac{N+S+M+E}{K_e}\right) E.
\end{aligned}
\tag{S6}
$$

We also explored the possibilities in which $r_n = 0$ or $r_m = 0$. In those cases we adapted the model in **equation S6** such that the state variables N and M had the forms $\frac{dN}{dt} = \lambda_f P + \lambda_s S - \hat{d}_n N$ and $\frac{dM}{dt} = \lambda_e P - \hat{d}_m M$, respectively.

We defined the statistical form of each parameter in $\Psi_j^{(1)}$ by using different functional forms. In complete detail:

- Parameters $\hat{r}_p^j, \hat{r}_n^j, \hat{r}_m^j, \hat{r}_e^j, \lambda_f^j, \lambda_e^j, \lambda_n^j, \lambda_s^j, \lambda_m^j, \hat{d}_n, \hat{d}_m$ were modeled as $\psi_j = \bar{\psi} e^{\eta_j}$.
- Parameters $\hat{d}_w$ were modeled as $\psi_j = \lambda_w(1 + \bar{\psi} e^{\eta_j})$, with $w \in [n, m]$.
- For K_p^j we used $10^{\psi_j} = 10^{\bar{\psi}+\eta_j}$.
- For $K_n^j, K_s^j, K_m^j, K_e^j$ we explored models with form $10^{\psi_j} = 10^{\bar{\psi}+\eta_j}$ or $10^{\psi_j} = 10^{K_p^j - \bar{\psi} e^{\eta_j}}$.
- We assumed that the initial values for each variable for each animal in the transplant group, $v_j(t_0)$, had a model with form $\psi_j = 10^{\bar{\psi}+\eta_j}$. For each animal in the control group we assumed the variables v to be in steady state at t_0 (see below).
- Other parameters where fixed for all animals as described in **Table 1** in the main text.

When simulating the model we assumed that t_0=0 represents the time of transplantation. For the transplant group we assumed that at t_0 the system is in a transient stage due to total body irradiation (TBI) with fixed total number of transplanted cells, $T(t_0) = 4 \times 10^7$ cells and fixed number of cells in the bone marrow/thymus compartment $P(t_0) = 0$. The number of cells in other compartments had a small value greater than zero, with distribution as described above. For the control group we used $t_0 = 0$ at a similar time relative to the transplant group on cART. Since the control group did not have any transplantation or TBI, we assumed $T(t_0) = 0$ and a system in steady state. Therefore, each state variable initial value was given by the following equations:

$$
\begin{aligned}
T(t_0) &= 0 \\
P(t_0) &= \frac{q_2 q_3 q_4 K_p}{(q_1+1) q_3 q_4 + q_2 (q_4+1)} \\
N(t_0) &= \frac{q_1 q_3 q_4 K_p}{(q_1+1) q_3 q_4 + q_2 (q_4+1)} \\
S(t_0) &= \frac{q_3 q_4 K_p}{(q_1+1) q_3 q_4 + q_2 (q_4+1)} \\
M(t_0) &= \frac{q_4 K_p}{\frac{(q_1+1) q_3 q_4}{q_2} + q_4 + 1} \\
E(t_0) &= \frac{K_p}{\frac{(q_1+1) q_3 q_4}{q_2} + q_4 + 1}
\end{aligned}
\tag{S7}
$$

Where $q_1 = \frac{\hat{r}_s}{\lambda_n}\left(\frac{K_p}{K_s} - 1\right)$, $q_2 = \frac{\hat{r}_n}{\lambda_f}\left(\frac{\hat{r}_s}{\lambda_n}\left(\frac{K_p}{K_n} - 1\right)\left(\frac{K_p}{K_s} - 1\right) - \lambda_s\right)$, $q_3 = \frac{\hat{r}_m}{\lambda_e}\left(\frac{K_p}{K_m} - 1\right)$ and $q_4 = \frac{\hat{r}_e}{\lambda_m}\left(\frac{K_p}{K_e} - 1\right)$. Note that parameters $\lambda_n, \lambda_f, \lambda_e, \lambda_m, K_s, K_n, K_m$, and K_e cannot be equal to zero.

For each instance of the model in **equation S6** we fit to 554 T cell observations from all animals simultaneously using a maximum likelihood approach. We estimated the standard deviation of the measurement error for the observations, and each parameter fixed effects and standard deviation of the random effects as described before.

2.3 Model selection

We listed different competing instances of the model in **equation S6** with different mechanistic and statistical assumptions as presented in **Table S1.** For best fit of the different possible versions of the models we computed the log-likelihood ($\log \mathcal{L}$) and the Akaike Information Criteria (AIC):

$$
AIC = -2 \log \mathcal{L} + 2l, \tag{S8}
$$

where l is the number of parameters estimated[2]. We assume models are equivalently supported by the data if the difference between their AIC values is less than two[2].

During model building we explored the following mechanistic hypotheses besides the full model:

- CD4$^+$CCR5$^+$ do not downregulate CCR5 ($\lambda_s = 0$).
- CD4$^+$CCR5$^-$ do not proliferate in a lymphopenic enviroment ($r_n = 0$).
- CD4$^+$CCR5$^-$ are long-lived in a lymphopenic enviroment ($d_n = 0$).
- CD8$^+$ T_{naive} and T_{CM} do not proliferate in a lymphopenic enviroment ($r_m = 0$).
- Thymic export of naive CD4$^+$ and CD8$^+$ T cells do not differ significantly ($\lambda_f = \lambda_e = \lambda_p$).

We evaluated single or combination of these mechanistic hypotheses along with different parameter's random effects distributions as listed in **Table S1** using AIC. From **Table S1** we found two models with similar support (row 16 and 19). These two models shared the following mechanistic assumptions: (1) $CD4^+CCR5^+$ do not downregulate CCR5, (2) $CD4^+CCR5^-$ do not proliferate in a lymphopenic enviroment, and (3) thymic export of naive $CD4^+$ and $CD8^+$ T cells do not differ significantly ($\lambda_f = \lambda_e = \lambda_p$). We selected the one that assumes that $CD8^+$ T_{CM} or T_N proliferate in a lymphopenic state (row 16) as literature seems to favor this possibility[3,4]. This 'best' model as found through AIC selection had the form:

$$\begin{aligned}
\frac{dT}{dt} &= -k_e T \\
\frac{dP}{dt} &= k_e T + \hat{r}_p \left(1 - \frac{N+S+M+E}{K_p}\right) P \\
\frac{dN}{dt} &= \lambda_p P - \hat{d}_n N \\
\frac{dS}{dt} &= \lambda_n N + \hat{r}_s \left(1 - \frac{N+S+M+E}{K_s}\right) S \\
\frac{dM}{dt} &= \lambda_p P + \hat{r}_m \left(1 - \frac{N+S+M+E}{K_m}\right) M \\
\frac{dE}{dt} &= \lambda_m M + \hat{r}_e \left(1 - \frac{N+S+M+E}{K_e}\right) E.
\end{aligned} \tag{S9}$$

with $C = M + E$ and $\lambda_p = \lambda_e = \lambda_f$.

3 Notes on fitting T cell and Viral load dynamics before and after ATI

3.1 Mathematical modeling.

For the fits of the T cell and viral dynamics after ATI we added a model for the observed plasma viral load V and we also assumed that $CD4^+CCR5^+$ T cells include infected cells. Now, we define the vector for the state variables $v^{(2)}$ as

$$v^{(2)} = \{R, N, C, M, E, V\}, \tag{S10}$$

with R indicating the observed blood $CD4^+CCR5^+$ T cell concentration, V indicating the observed plasma viral load, and the others state-variables as specified for $v^{(1)}$.

We modeled the kinetics of $v^{(2)}$ by adapting the model in **equation S9**. This model is based on the following assumptions. Susceptible cells, S are infected by the virus, V, at rate β. We modeled cART by reducing β to zero, and ATI by assuming $\beta > 0$ with delay Δ_t after interruption. We assumed a fraction τ of the infected cells produce virus, I_p, and the other fraction become unproductively infected, I_u. Only I_p cells arise from activation of a steady set of latently infected cells at rate $\xi\bar{L}$.

All infected cells die at rate δ_I. I_p cells produce virus at a rate π per cell, that is cleared at rate γ. CD8$^+$ M cells proliferate in the presence of infection with maximum rate ω. A fraction f of these cells become SHIV-specific CD8$^+$ effector T cells, E_h, that are removed at a rate d_h. These effector cells may reduce virus production or infectivity by $\frac{1}{1+\theta E_h}$, or $\frac{1}{1+\phi E_h}$, respectively. For cell growth the total number of competing cells is given by $A = N + S + I_p + I_u + M + E + E_h$. We assumed that non-susceptible CD4$^+$ T cells may upregulate CCR5 and replenish the susceptible pool with rate ω_4. Under these assumptions the model in **equation S9** becomes

$$\begin{aligned}
\frac{dT}{dt} &= -k_e T \\
\frac{dP}{dt} &= k_e T + \hat{r}_p \left(1 - \frac{A}{K_p}\right) P \\
\frac{dN}{dt} &= \lambda_p P - \hat{d}_n N - \omega_4 \frac{I_p + I_u}{1 + \frac{I_p + I_u}{I_{50}}} N \\
\frac{dS}{dt} &= \lambda_n N + \hat{r}_s \left(1 - \frac{A}{K_s}\right) S - \frac{1}{1 + \phi E_h} \beta V S + \omega_4 \frac{I_p + I_u}{1 + \frac{I_p + I_u}{I_{50}}} N \\
\frac{dI_p}{dt} &= \frac{1}{1 + \phi E_h} \tau \beta V S - \delta_I I_p + \xi L \\
\frac{dI_u}{dt} &= \frac{1}{1 + \phi E_h} (1 - \tau) \beta V S - \delta_I I_u \\
\frac{dV}{dt} &= \frac{1}{1 + \theta E_h} \pi I_p - \gamma V \\
\frac{dM}{dt} &= \lambda_p P + r_m \left(1 - \frac{A}{K_m}\right) M + \omega_8 (1 - f) \frac{I_p + I_u}{1 + \frac{I_p + I_u}{I_{50}}} M \\
\frac{dE}{dt} &= \lambda_m M + \hat{r}_e \left(1 - \frac{A}{K_e}\right) E \\
\frac{dE_h}{dt} &= \omega_8 f \frac{I_p + I_u}{1 + \frac{I_p + I_u}{I_{50}}} M - d_h E_h
\end{aligned} \tag{S11}$$

with $A = N + S + I_p + I_u + M + E + E_h$ and $\beta = 0$ if $t < (t_{ATI} + \Delta_t)$. Here, t_{ATI} is the time of cART interruption relative to the time of transplant. We defined the total number of CD4$^+$CCR5$^+$ T cells as $R = S + I_p + I_u$.

We also explored the possibility in which SHIV-specific CD8$^+$ effector T cells proliferate in the absence of infected cells (i.e., by homeostatic proliferation), and have the same death rate as non-SHIV-specific CD8$^+$ T effector cells ($d_e = d_h$). In this case we defined the equation for SHIV-specific CD8$^+$ T effector cells as

$$\frac{dE_h}{dt} = \hat{r}_e \left(1 - \frac{A}{K_e}\right) E_h + \omega_8 f \frac{I_p + I_u}{1 + \frac{I_p + I_u}{I_{50}}} M \tag{S12}$$

3.2 Model fitting

For this model we defined the parameter set $\Psi_j^{(2)}$ by adding to the parameters in the previous section the parameters relative to virus dynamics (i.e., $\Psi_j^{(2)} = \{\Psi_j^{(1)}, \phi^j, \theta^j, \beta^j, \omega_4^j, \omega_8^j, I_{50}^j, \Delta_t^j, d_h^j\}$). For parameters ϕ^j, θ^j, β^j, ω_4^j, ω_8^j, and I_{50}^j we used a probabilistic model with form $10^{\psi_j} = 10^{\bar{\psi}+\eta_j}, \eta_j \sim \mathcal{N}\left(0, \sigma_\psi^2\right)$; and for Δ_t^j and d_h^j we used $\psi_j = \bar{\psi} e^{\eta_j}, \eta_j \sim \mathcal{N}\left(0, \sigma_\psi^2\right)$. Other parameters where fixed for all animals as described in **Table 1** in the main text.

We fit each model to 1101 data points (T cell counts and plasma viral load observations) from all animals simultaneously using a maximum likelihood approach in Monolix assuming that each observation v_{ij} is independent for each variable in $v^{(2)}$, for each animal j at each time point t_i. For the transplant group we assumed that $t_0 = 0$ represents the time of transplant and had the same assumptions as before for the initial values of the state variables *T*, *P*, *S*, *N*, *M*, and *E*. For state variables I_p, I_u and V we assume they were the same for both control and transplant groups using the equations shown below. For the control group, the initial values were given by the following equations:

$$
\begin{aligned}
T(t_0) &= 0 \\
P(t_0) &= \frac{q_2 q_3 q_4 K_p}{(q_1+1) q_3 q_4 + q_2 (q_4+1)} \\
N(t_0) &= \frac{q_1 q_3 q_4 K_p}{(q_1+1) q_3 q_4 + q_2 (q_4+1)} \\
S(t_0) &= \frac{q_3 q_4 K_p}{(q_1+1) q_3 q_4 + q_2 (q_4+1)} \\
M(t_0) &= \frac{q_4 K_p}{\frac{(q_1+1) q_3 q_4}{q_2} + q_4 + 1} \\
E(t_0) &= \frac{K_p}{\frac{(q_1+1) q_3 q_4}{q_2} + q_4 + 1} \\
E_h(t_0) &= \frac{1}{d_h}\left(\frac{\omega_8 f M(t_0) I_p(t_0)}{1+\frac{I_p(t_0)}{I_{50}}}\right) \\
I_p(t_0) &= \frac{\xi L}{\delta_I} \\
I_u(t_0) &= 0 \\
V(t_0) &= \frac{\pi I_p(t_0)}{\gamma}.
\end{aligned}
\tag{S13}
$$

Here $q_1 = \frac{\hat{r}_s}{\lambda_n + \frac{\omega_4 I_p(t_0)}{1+\frac{I_p(t_0)}{I_{50}}}}\left(\frac{K_p}{K_s} - 1\right)$, $q_2 = \frac{q_1}{\lambda_p}\left(\frac{\omega_4 I_p(t_0)}{1+\frac{I_p(t_0)}{I_{50}}} + \hat{d}_n\right)$, $q_3 = \frac{1}{\lambda_p}\left(\hat{r}_m\left(\frac{K_p}{K_m} - 1\right) - \frac{\omega_8 (1-f) I_p(t_0)}{1+\frac{I_p(t_0)}{I_{50}}}\right)$ and $q_4 = \frac{\hat{r}_e}{\lambda_m}\left(\frac{K_p}{K_e} - 1\right)$.

3.3 Model selection

We used model selection theory using AIC as presented previously. During model building we explored the following mechanistic hypotheses besides the full model:

- SHIV-specific CD8$^+$ effector T cells do not affect virus infectivity ($\phi = 0$).
- SHIV-specific CD8$^+$ effector T cells do not affect virus processes after integration ($\theta = 0$).
- CD4$^+$CCR5$^-$ are not activated/do not express CCR5 in the presence of infected cells ($\omega_4 = 0$).
- SHIV-specific CD8$^+$ effector T cells proliferate in the absence of infected cells and have the same death rate as non-SHIV-specific CD8$^+$ T effector cells ($d_e = d_h$).

We evaluated single or combination of these mechanistic hypotheses along with different parameter's random effects distributions as listed in **Table S2** using AIC. From **Table S2** we found that the model that most parsimoniously explains the whole data set includes the following: (1) SHIV-specific CD8$^+$ effector T cells do not affect virus infectivity, (2) CD4$^+$CCR5$^-$ express CCR5 in the presence of infected cells and (3) SHIV-specific CD8$^+$ effector T cells do not proliferate in the absence of infected cells. This model has the form:

$$
\begin{aligned}
\frac{dT}{dt} &= -k_e T \\
\frac{dP}{dt} &= k_e T + \hat{r}_p \left(1 - \frac{A}{K_p}\right) P \\
\frac{dN}{dt} &= \lambda_p P - \hat{d}_n N - \omega_4 \frac{I_p + I_u}{1 + \frac{I_p + I_u}{I_{50}}} N \\
\frac{dS}{dt} &= \lambda_n N + \hat{r}_s \left(1 - \frac{A}{K_s}\right) S - \beta V S + \omega_4 \frac{I_p + I_u}{1 + \frac{I_p + I_u}{I_{50}}} N \\
\frac{dI_p}{dt} &= \tau \beta V S - \delta_I I_p + \xi L \\
\frac{dI_u}{dt} &= (1 - \tau) \beta V S - \delta_I I_u \\
\frac{dV}{dt} &= \frac{1}{1 + \theta E_h} \pi I_p - \gamma V \\
\frac{dM}{dt} &= \lambda_p P + r_m \left(1 - \frac{A}{K_m}\right) M + \omega_8 (1 - f_p) \frac{I_p + I_u}{1 + \frac{I_p + I_u}{I_{50}}} M \\
\frac{dE}{dt} &= \lambda_m M + \hat{r}_e \left(1 - \frac{A}{K_e}\right) E \\
\frac{dE_h}{dt} &= \omega_8 f \frac{I_p + I_u}{1 + \frac{I_p + I_u}{I_{50}}} M - d_h E_h.
\end{aligned}
\tag{S14}
$$

4 Full model including gene-edited cells.

We adapted the model to include cells that are CCR5 gene-modified: CCR5 gene-modified- transplanted HSPCs T_p, T cell progenitor cells in BM/thymus P_p, and blood CD4$^+$CCR5$^-$ T cells N_p. Here, $T_p(t_0) = 4 \times 10^7 f_p$ and $T(t_0) = 4 \times 10^7 (1 - f_p)$. Thus, the complete model had the form:

$$
\begin{aligned}
\frac{dT_p}{dt} &= -k_e T_p \\
\frac{dP_p}{dt} &= k_e T_p + \hat{r}_p \left(1 - \frac{A}{K_p}\right) P_p \\
\frac{dN_p}{dt} &= \lambda_p P_p - \hat{d}_n N_p \\
\frac{dT}{dt} &= -k_e T \\
\frac{dP}{dt} &= k_e T + \hat{r}_p \left(1 - \frac{A}{K_p}\right) P \\
\frac{dN}{dt} &= \lambda_p P - d_n N - \omega_4 \frac{I_p + I_u}{1 + \frac{I_p + I_u}{I_{50}}} N \\
\frac{dS}{dt} &= \lambda_n N + \hat{r}_s \left(1 - \frac{A}{K_s}\right) S - \beta V S + \omega_4 \frac{I_p + I_u}{1 + \frac{I_p + I_u}{I_{50}}} N \\
\frac{dI_p}{dt} &= \tau \beta V S - \delta_I I_p + \xi L \\
\frac{dI_u}{dt} &= (1 - \tau) \beta V S - \delta_I I_u \\
\frac{dV}{dt} &= \frac{1}{1 + \theta E_h} \pi I_p - \gamma V \\
\frac{dM}{dt} &= \lambda_p (P + P_p) + \hat{r}_m \left(1 - \frac{A}{K_m}\right) M + \omega_8 (1 - f_p) \frac{I_p + I_u}{1 + \frac{I_p + I_u}{I_{50}}} M \\
\frac{dE}{dt} &= \lambda_m M + \hat{r}_e \left(1 - \frac{A}{K_e}\right) E \\
\frac{dE_h}{dt} &= \omega_8 f \frac{I_p + I_u}{1 + \frac{I_p + I_u}{I_{50}}} M - d_h E_h
\end{aligned}
\tag{S15}
$$

where $A = N + S + I_p + I_u + M + E + E_h$, $\beta = 0$ if $t < (ATI + \Delta_t)$, and total number of CD4$^+$CCR5$^+$ T cells as $S + I_p + I_u$.

5 Supplementary Figures

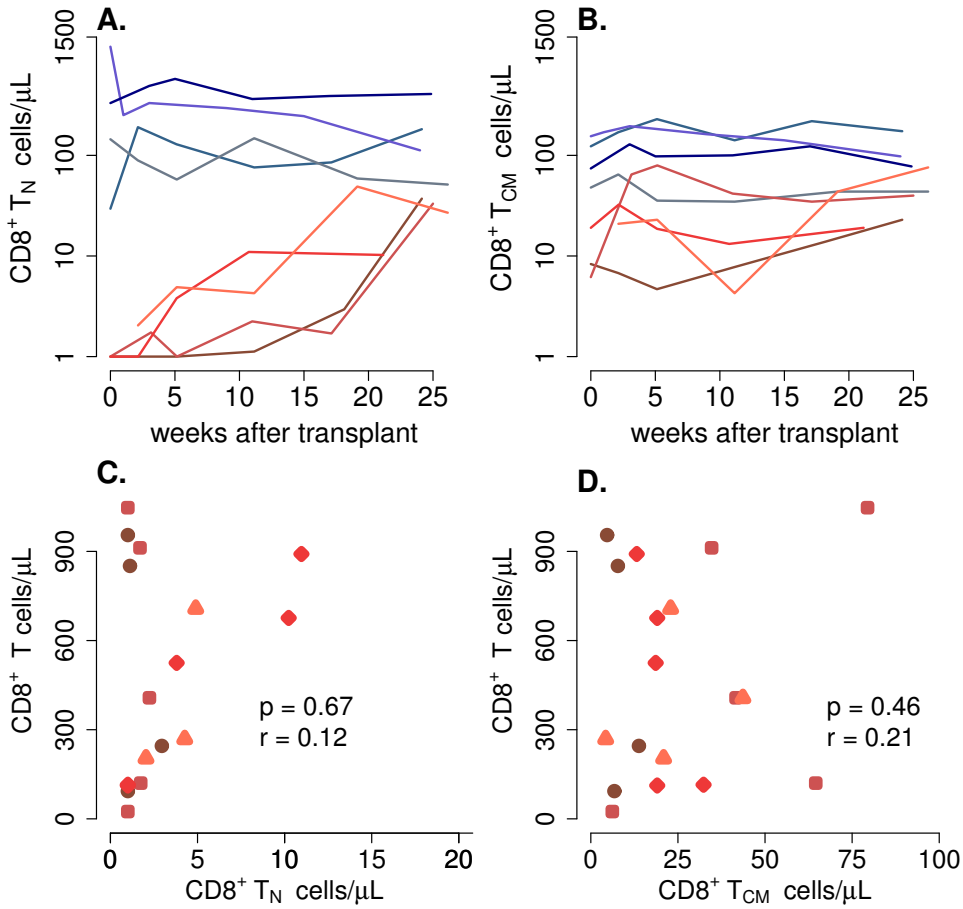

Supplementary Fig 1. CD8$^+$ T cell subset kinetics after transplant and before ATI (No transplant for the animals in the control group). Blood cell counts for **(A)** CD8$^+$ T_N and **(B)** CD8$^+$ T_{CM} cells (blue lines: control group, red lines: transplant group). Scatterplots comparing the total CD8$^+$ T cell concentrations vs **(C)** CD8$^+$ T_N and **(D)** CD8$^+$ T_{CM} cells over time from animals in the transplant group (p-value computed using repeated measures correlation test).

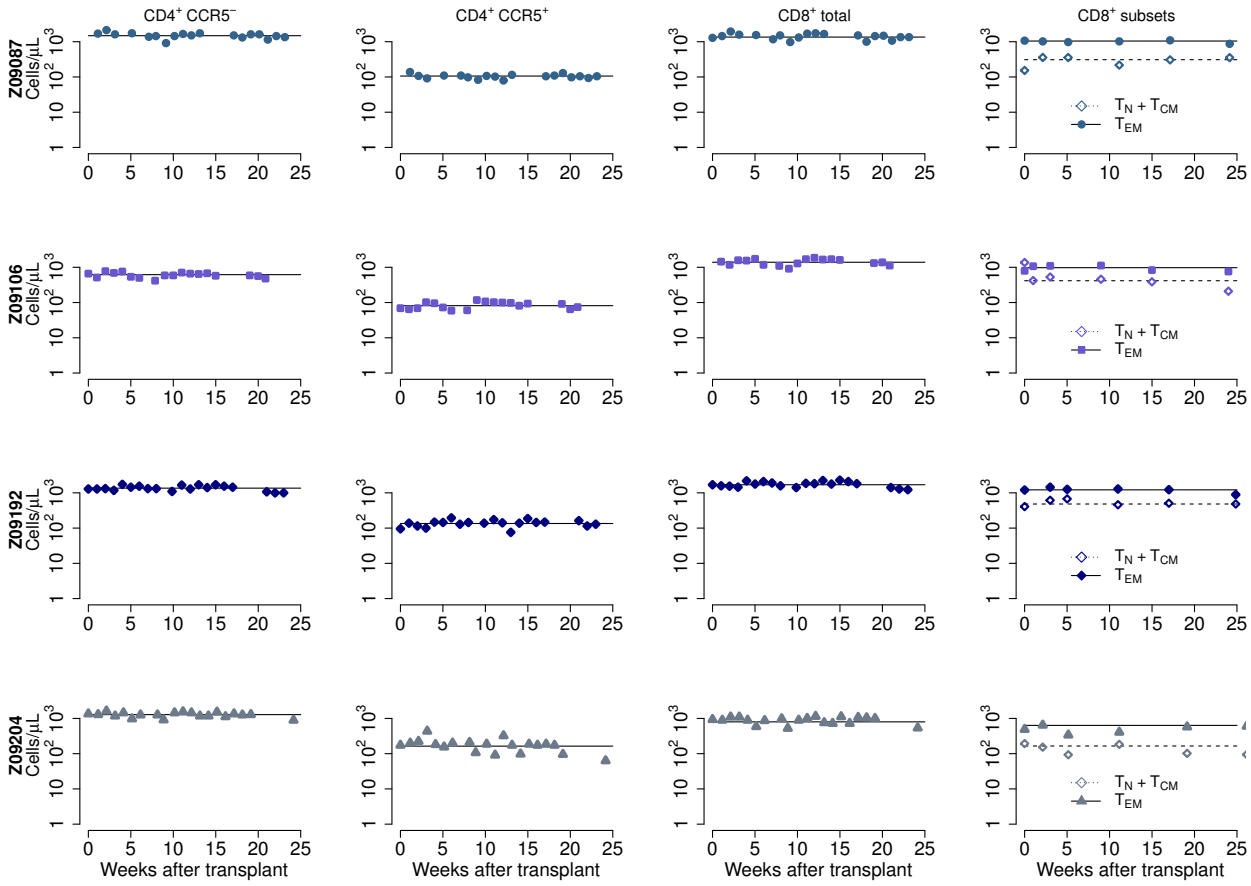

Supplementary Fig 2. Best fits of the model in **equation S9** to all blood T cell subsets before ATI for the control group. Each row is one animal.

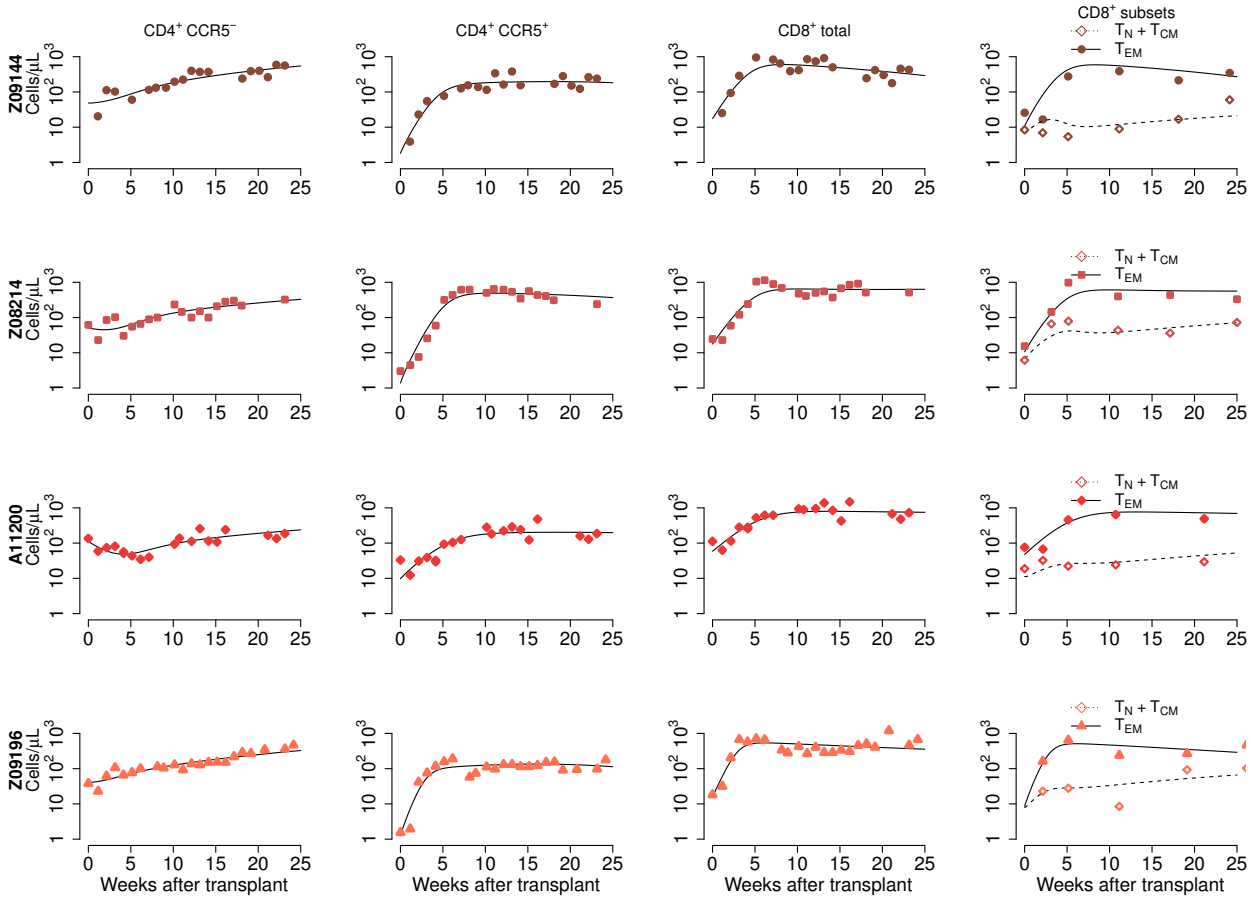

Supplementary Fig 3. Best fits of the model in **equation S9** to all blood T cell subsets before ATI for the transplant group. Each row is one animal.

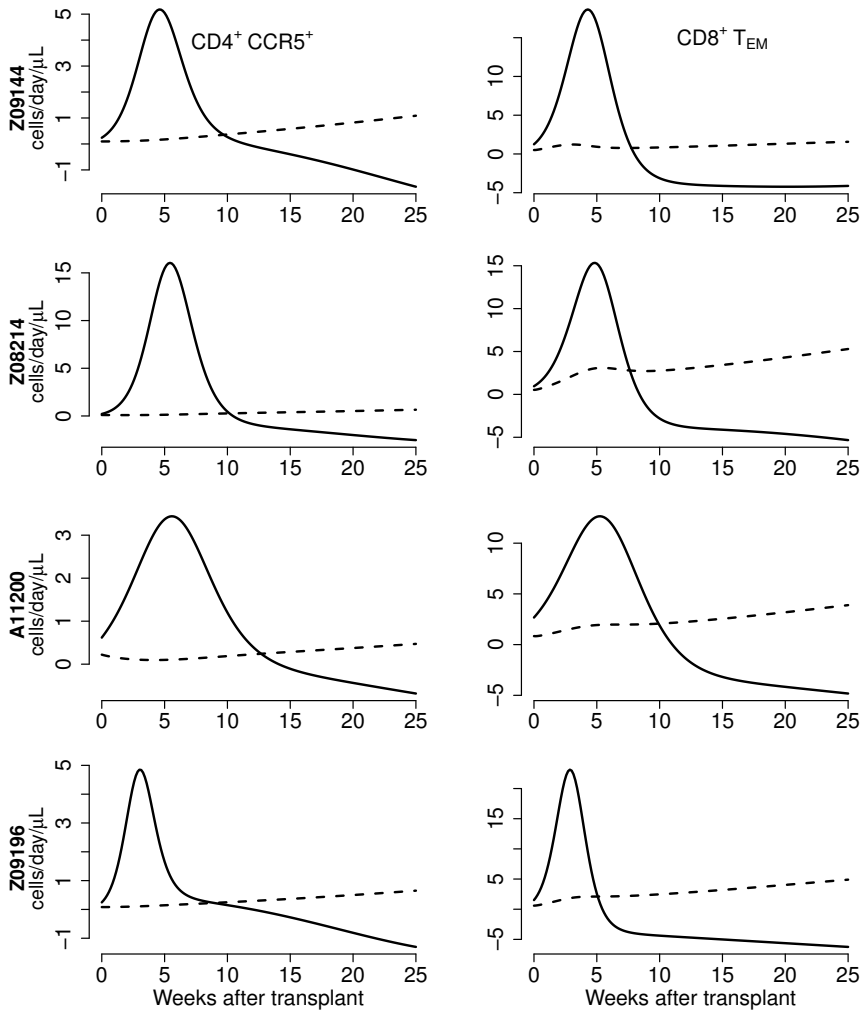

Supplementary Fig 4. Predictions of the model in **equation S9** for the contributors to cell expansion in $CD4^+CCR5^+$ T and $CD8^+$ T_{EM} cells in animals from the transplant group. Solid lines represent the total amount of cells that proliferate over time ($r_s \left(1 - \frac{N+S+M+E}{K_s}\right) S$ and $r_e \left(1 - \frac{N+S+M+E}{K_e}\right) E$ for $CD4^+CCR5^+$ T and $CD8^+$ T_{EM} cells, respectively). Dashed lines indicate the number of exogenous cells differentiated from T_{naive} and T_{CM} that upregulate CCR5 over time ($\lambda_n N$ and $\lambda_m M$ for $CD4^+CCR5^+$ T and $CD8^+$ T_{EM} cells, respectively). Each row is one animal.

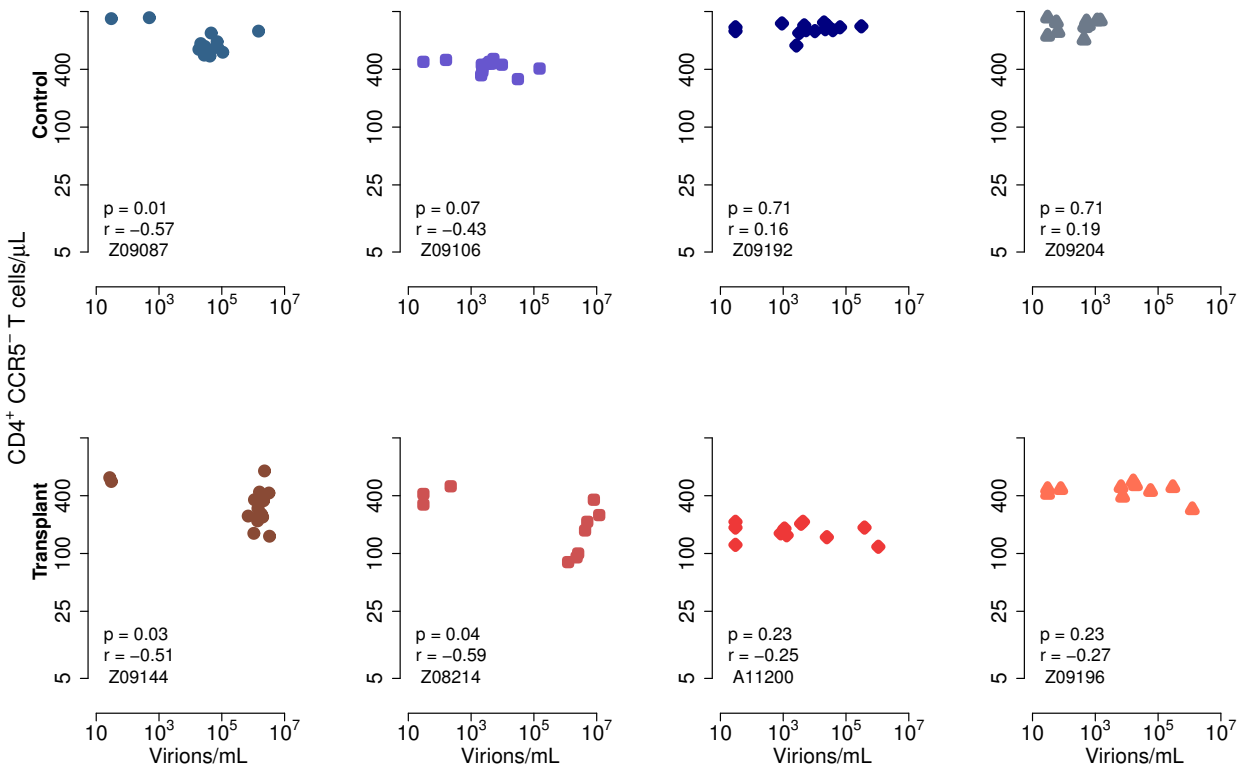

Supplementary Fig 5. Correlations between viral load and $CD4^{+}CCR5^{-}$ T cells over time in each animal post-ATI. Each panel shows the timepoints post-ATI for each animal. P-values in each panel were calculated using Spearman's rank test for all time points post-ATI for the corresponding animal.

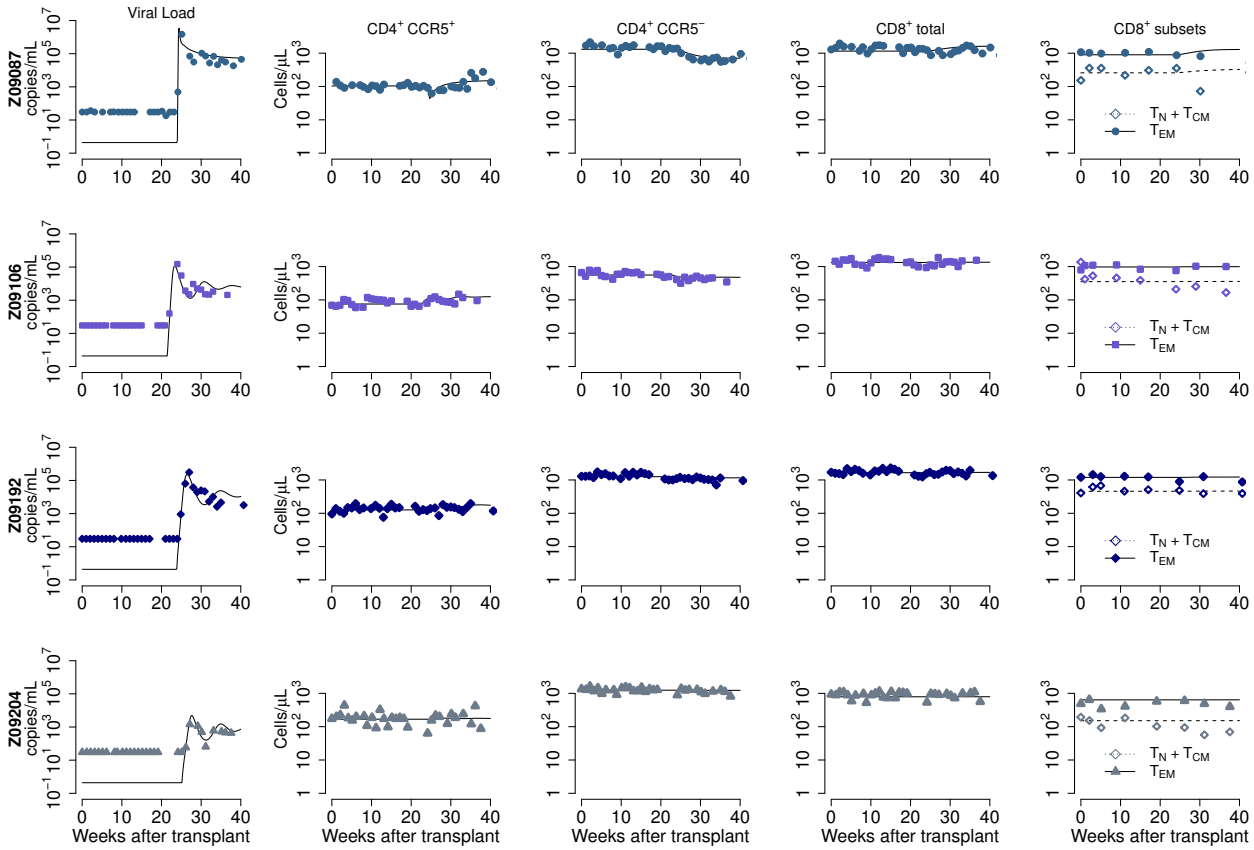

Supplementary Fig 6. Best fits of the model in **equation S14** to all blood T cell subsets before/after ATI for the control group. Each row is one animal.

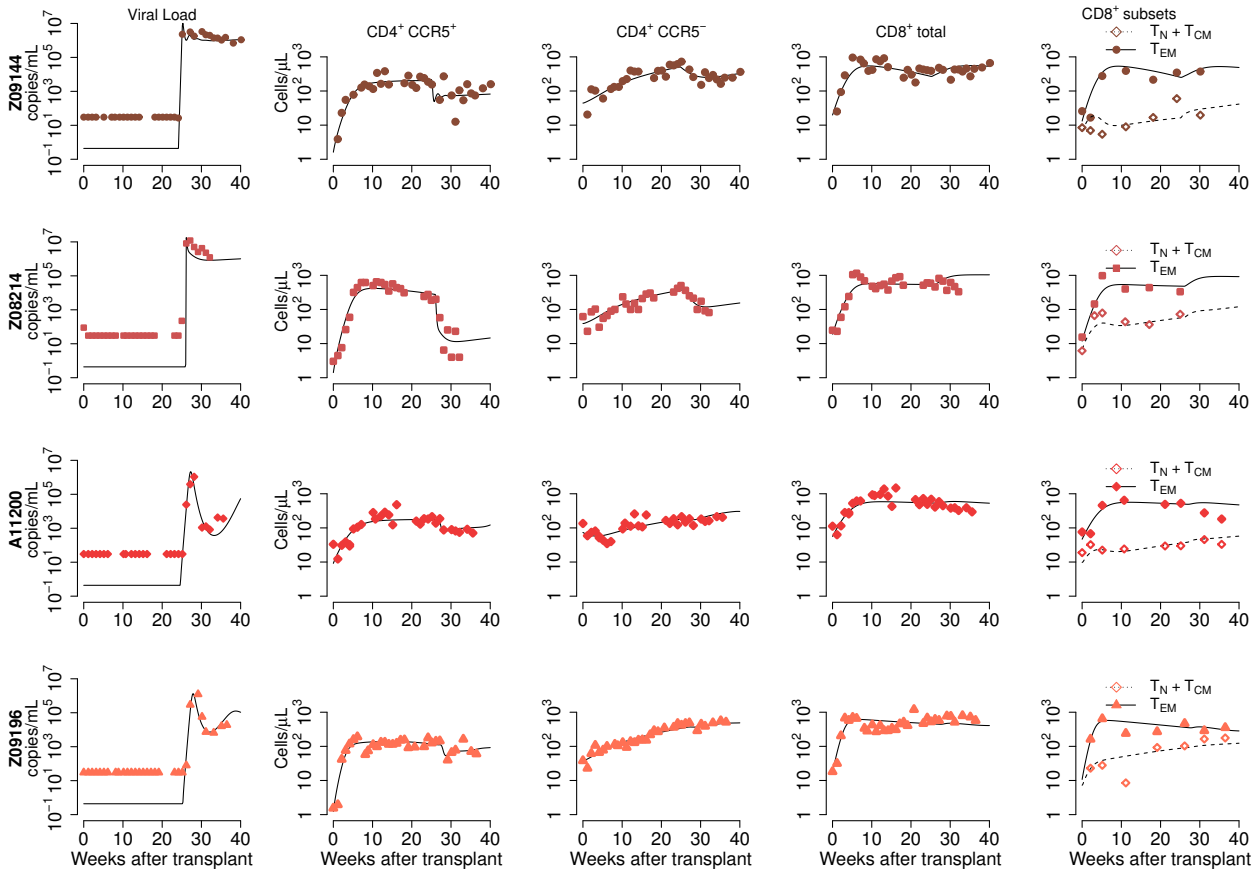

Supplementary Fig 7. Best fits of the model in **equation S14** to all blood T cell subsets before/after ATI for the transplant group. Each row is one animal.

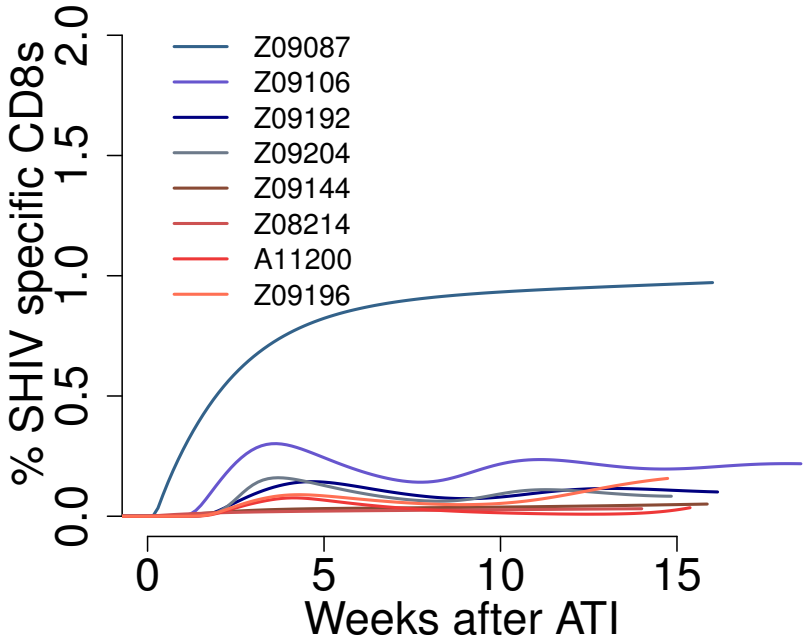

Supplementary Fig 8. Prediction of the model in **equation S14** for the proportion of SHIV-specific CD8+ T cells over time during ATI $\left(\%\text{SHIV-specific CD8s} = 100 \times \frac{E_h}{E_h+M+E}\right)$. Transplanted macaques in red. Controls in blue.

6 Supplementary Tables

Table 1: Competing models for fitting T cell reconstitution with respective AIC values. Best fit in bold-red (lowest AIC). In all cases, $\eta_j \sim \mathcal{N}\left(0, \sigma_\psi^2\right)$. $\forall j$ indicates 'for all animals'.

#	**Description and mathematical/fitting properties**	**AIC**
1	Full model. $K_n^j, K_s^j, K_m^j, K_e^j$ are modeled as $10^{\psi_j} = 10^{K_p^j - \bar{\psi} e^{\eta_j}}$.	-276.5
2	Full model. $K_n^j, K_s^j, K_m^j, K_e^j$ are modeled as $10^{\psi_j} = 10^{\bar{\psi} + \eta_j}$.	-51.8
3	$\lambda_s = 0\ \forall j$. $K_n^j, K_s^j, K_m^j, K_e^j$ are modeled as $10^{\psi_j} = 10^{\bar{\psi} + \eta_j}$.	-250.3
4	$\lambda_s = 0\ \forall j$. $K_n^j, K_s^j, K_m^j, K_e^j$ are modeled as $10^{\psi_j} = 10^{K_p^j - \bar{\psi} e^{\eta_j}}$.	-280.1
5	$r_n = 0$ and $d_n = 0\ \forall j$. $K_n^j, K_s^j, K_m^j, K_e^j$ are modeled as $10^{\psi_j} = 10^{K_p^j - \bar{\psi} e^{\eta_j}}$.	-279.7
6	$\lambda_e = \lambda_f$, $r_n = 0$, and $d_n = 0\ \forall j$. K_s^j, K_m^j, K_e^j are modeled as $10^{\psi_j} = 10^{K_p^j - \bar{\psi} e^{\eta_j}}$.	-279.3
7	$\lambda_e = \lambda_f$, $r_n = 0$, $d_n = 0$, and $\lambda_s = 0\ \forall j$. K_s^j, K_m^j, K_e^j are modeled as $10^{\psi_j} = 10^{K_p^j - \bar{\psi} e^{\eta_j}}$.	-260.5
8	$r_n = 0, d_n = 0$, and $\lambda_s = 0\ \forall j$. K_s^j, K_m^j, K_e^j are modeled as $10^{\psi_j} = 10^{K_p^j - \bar{\psi} e^{\eta_j}}$.	-261.9
9	$r_n = 0\ \forall j$. $\hat{d}_n^j$ is modeled as $\hat{d}_n^j = \lambda_n \left(1 + \bar{\psi} e^{\eta_j}\right)$. K_s^j, K_m^j, K_e^j are modeled as $10^{\psi_j} = 10^{K_p^j - \bar{\psi} e^{\eta_j}}$.	-278.3
10	$\lambda_e = \lambda_f$ and $r_n = 0\ \forall j$. $\hat{d}_n^j$ is modeled as $\hat{d}_n^j = \lambda_n \left(1 + \bar{\psi} e^{\eta_j}\right)$. K_s^j, K_m^j, K_e^j are modeled as $10^{\psi_j} = 10^{K_p^j - \bar{\psi} e^{\eta_j}}$.	-276.5
11	$\lambda_s = 0$, $\lambda_e = \lambda_f$ and $r_n = 0\ \forall j$. $\hat{d}_n^j$ is modeled as $\hat{d}_n^j = \lambda_n \left(1 + \bar{\psi} e^{\eta_j}\right)$. K_s^j, K_m^j, K_e^j are modeled as $10^{\psi_j} = 10^{K_p^j - \bar{\psi} e^{\eta_j}}$.	-284.5
12	$\lambda_s = 0$ and $r_n = 0\ \forall j$. $\hat{d}_n^j$ is modeled as $\hat{d}_n^j = \lambda_n \left(1 + \bar{\psi} e^{\eta_j}\right)$. K_s^j, K_m^j, K_e^j are modeled as $10^{\psi_j} = 10^{K_p^j - \bar{\psi} e^{\eta_j}}$.	-281.0
13	$\lambda_s = 0$, $\lambda_e = \lambda_f$ and $r_n = 0\ \forall j$. $\hat{d}_n^j$ is modeled as $\hat{d}_n^j = \lambda_n \left(1 + \bar{\psi} e^{\eta_j}\right)$. K_s^j, K_m^j, K_e^j are modeled as $10^{\psi_j} = 10^{K_p^j - \bar{\psi}}$, $\sigma_\psi = 0$.	-291.2
14	$\lambda_s = 0$ and $r_n = 0\ \forall j$. $\hat{d}_n^j$ is modeled as $\hat{d}_n^j = \lambda_n \left(1 + \bar{\psi} e^{\eta_j}\right)$. K_s^j, K_m^j, K_e^j are modeled as $10^{\psi_j} = 10^{K_p^j - \psi}$, $\sigma_\psi = 0$.	-289.5
15	$\lambda_s = 0$, $\lambda_e = \lambda_f$ and $r_n = 0\ \forall j$. $\hat{d}_n^j$ is modeled as $\hat{d}_n^j = \lambda_n \left(1 + \bar{\psi} e^{\eta_j}\right)$. K_s^j, K_m^j, K_e^j are modeled as $10^{\psi_j} = 10^{K_p^j - \bar{\psi}}$, $\sigma_\psi = 0$. $\lambda_n, \lambda_f, \lambda_e, \lambda_m$ are modeled as $\psi_j = \bar{\psi}$, $\eta_j = 0$.	-297.7
16	$\lambda_s = 0$, $\lambda_e = \lambda_f$ and $r_n = 0\ \forall j$. $\hat{d}_n^j$ is modeled as $\hat{d}_n^j = \lambda_n \left(1 + \bar{\psi} e^{\eta_j}\right)$. K_s^j, K_m^j, K_e^j are modeled as $10^{\psi_j} = 10^{K_p^j - \bar{\psi}}$, $\sigma_\psi = 0$. $r_p, \lambda_n, \lambda_f, \lambda_e, \lambda_m$ are modeled as $\psi_j = \bar{\psi}$, $\sigma_\psi = 0$.	**-299.9**
17	$\lambda_e = \lambda_f$, $r_n = 0$ and $r_m = 0\ \forall j$. $\hat{d}_n^j$ is modeled as $\hat{d}_n^j = \lambda_n \left(1 + \bar{\psi} e^{\eta_j}\right)$. $\hat{d}_m^j$ is modeled as $\hat{d}_m^j = \lambda_m \left(1 + \bar{\psi} e^{\eta_j}\right)$. K_s^j, K_e^j are modeled as $10^{\psi_j} = 10^{K_p^j - \bar{\psi} e^{\eta_j}}$.	-281.6
18	$\lambda_s = 0$, $\lambda_e = \lambda_f$, $r_n = 0$ and $r_m = 0\ \forall j$. $\hat{d}_n^j$ is modeled as $\hat{d}_n^j = \lambda_n \left(1 + \bar{\psi} e^{\eta_j}\right)$. $\hat{d}_m^j$ is modeled as $\hat{d}_m^j = \lambda_m \left(1 + \bar{\psi} e^{\eta_j}\right)$. K_s^j, K_e^j are modeled as $10^{\psi_j} = 10^{K_p^j - \bar{\psi} e^{\eta_j}}$.	-285.2
19	$\lambda_s = 0, \lambda_e = \lambda_f, r_n = 0$ and $r_m = 0\ \forall j$. $\hat{d}_n^j$ is modeled as $\hat{d}_n^j = \lambda_n \left(1 + \bar{\psi} e^{\eta_j}\right)$. $\hat{d}_m^j$ is modeled as $\hat{d}_m^j = \lambda_m \left(1 + \bar{\psi} e^{\eta_j}\right)$. K_s^j, K_e^j are modeled as $10^{\psi_j} = 10^{K_p^j - \psi}$, $\sigma_\psi = 0$. $r_p, \lambda_n, \lambda_f, \lambda_e, \lambda_m$ are modeled as $\psi_j = \bar{\psi}$, $\sigma_\psi = 0$.	-298.9

Table 2: Competing models for fitting T cell and viral dynamics using the best model in **Table S1**, with AIC values. Best fit in bold-red (lowest AIC).

	Assumptions on Ψ_j	**AIC**
1	$\theta = \phi = 1$ for all animals.	-185.7
2	$\theta = 1$, $\phi = 0$ for all animals.	-197.2
3	$\theta = 0$, $\phi = 1$ for all animals.	-183.3
4	$\theta = 1$, $\phi = 0$ for all animals. d_h^j is modeled as $\psi_j = \bar{\psi}$, $\sigma_\psi = 0$.	-200.3
5	$\theta = 0$, $\phi = 1$ for all animals. d_h^j is modeled as $\psi_j = \bar{\psi}$, $\sigma_\psi = 0$.	-186.3
6	$\phi = 0$ for all animals. d_h^j is modeled as $\psi_j = \psi$, $\sigma_\psi = 0$. θ^j is modeled as $10^{\psi_j} = 10^{\bar{\psi}}$, $\sigma_\psi = 0$.	-196.4
7	$\theta = 0$ for all animals. d_h^j is modeled as $\psi_j = \bar{\psi}$, $\sigma_\psi = 0$. ϕ^j is modeled as $10^{\psi_j} = 10^{\bar{\psi}}$, $\sigma_\psi = 0$.	-183.6
8	$\theta = 1$, $\phi = 0$ for all animals. d_h^j is modeled as $\psi_j = \bar{\psi}$, $\sigma_\psi = 0$. ω_4^j is modeled as $10^{\psi_j} = 10^{\bar{\psi}}$, $\sigma_\psi = 0$.	-200
9	$\theta = 1$, $\phi = 0$ for all animals. d_h^j is modeled as $\psi_j = \bar{\psi}$, $\sigma_\psi = 0$. I_{50}^j is modeled as $10^{\psi_j} = 10^{\bar{\psi}}$, $\sigma_\psi = 0$.	**-203.7**
10	$\theta = 1$, $\phi = 0$ for all animals. d_h^j is modeled as $\psi_j = \bar{\psi}$, $\sigma_\psi = 0$. β^j is modeled as $10^{\psi_j} = 10^{\bar{\psi}}$, $\sigma_\psi = 0$.	-127
11	$\theta = 1$, $\phi = 0$, and $\omega_4 = 0$ for all animals. d_h is modeled as $\psi_j = \bar{\psi}$, $\sigma_\psi = 0$.	-42
12	Adapted equation for E_h : $\frac{dE_h}{dt} = r_e \left(1 - \frac{A}{K_e}\right) E_h + \omega_8 f \frac{I_p + I_u}{1 + \frac{I_p + I_u}{I_{50}}} M$ $\theta = 1$, $\phi = 0$ for all animals.	-188.9
13	Adapted equation for E_h : $\frac{dE_h}{dt} = r_e \left(1 - \frac{A}{K_e}\right) E_h + \omega_8 f \frac{I_p + I_u}{1 + \frac{I_p + I_u}{I_{50}}} M$ $\theta = 0$, $\phi = 1$ for all animals.	-173.41
14	Adapted equation for E_h : $\frac{dE_h}{dt} = r_e \left(1 - \frac{A}{K_e}\right) E_h + \omega_8 f \frac{I_p + I_u}{1 + \frac{I_p + I_u}{I_{50}}} M$ $\phi = 0$ for all animals. θ^j is modeled as $10^{\psi_j} = 10^{\bar{\psi}}$, $\sigma_\psi = 0$.	-185.1
15	Adapted equation for E_h : $\frac{dE_h}{dt} = r_e \left(1 - \frac{A}{K_e}\right) E_h + \omega_8 f \frac{I_p + I_u}{1 + \frac{I_p + I_u}{I_{50}}} M$ $\theta = 0$ for all animals. ϕ^j is modeled as $10^{\psi_j} = 10^{\bar{\psi}}$, $\sigma_\psi = 0$.	-171.1

Table 3: Population parameter estimates for the fits of the model in **equation S9** (lowest AIC in **Table S1**) to the T cell reconstitution dynamics. RSE: relative standard error. Empty fields represent cases when the standard deviation of random effects, σ_ψ , was fixed to zero. Values of the fixed effects ($\bar{\psi}$) obtained for K_p, $N\left(t_0\right)$, $S\left(t_0\right)$, $M\left(t_0\right)$, and $E\left(t_0\right)$ had units of absolute cell counts in the model. The values shown here (and used when fitting to data) are in logarithmic scale due to the definition of ψ_j but were transformed after dividing to $5 \times 10^5 \mu$L, the assumed blood volume in macaques (the blood volume was calculated in the same way for all animals, assuming a blood:weight ratio of 100mL/Kg, and body weight of 5Kg). Red values represent a RSE greater than 100%, implying that the number of data points may not be enough to estimate those parameters.

Parameter	ψ	σ_ψ	% **RSE** ψ	% **RSE** σ_ψ
$\hat{r}_p$	0.05		22	
$\hat{r}_s$	0.12	0.35	18	28
$\hat{r}_m$	0.002	0.66	**1382**	38
$\hat{r}_e$	0.11	0.35	18	33
$\hat{d}_n$	13.8	0.76	59	34
λ_p	0.01		42	
λ_n	0.002		46	
λ_m	0.07		36	
K_p	3.2	0.19	1	25
K_s	0.07		40	
K_m	2.0		**294**	
K_e	0.09		32	
$N\left(t_0\right)$	1.8	0.18	1	42
$S\left(t_0\right)$	0.4	0.37	3	41
$M\left(t_0\right)$	0.9	0.15	2	120
$E\left(t_0\right)$	1.2	0.33	3	43
σ_N	0.16		6	
σ_S	0.12		6	
σ_C	0.15		6	
σ_E	0.19		11	
σ_M	0.23		12	

Table 4: Individual parameter estimates for the fits of the model in **equation S9** (lowest AIC in **Table S1**) to the T cell reconstitution dynamics. Values obtained for $K_p, N(t_0), S(t_0), M(t_0)$, and $E(t_0)$ had units of absolute cell counts in the model. The values shown here were transformed after dividing to $5 \times 10^5 \mu$L, the assumed blood volume in a pigtailed macaque (the blood volume was calculated in the same way for all animals, assuming a blood:weight ratio of 100mL/Kg, and body weight of 5Kg). Initial values for the control group where obtained from **equation S7**.

	Control				**Transplant**			
	Z09087	**Z09106**	**Z09192**	**Z09204**	**Z09144**	**Z08214**	**A11200**	**Z09196**
$\hat{r}_p^j$ [day^{-1}]	0.05	0.05	0.05	0.05	0.05	0.05	0.05	0.05
$\hat{r}_s^j$ [day^{-1}]	0.17	0.09	0.12	0.09	0.14	0.16	0.08	0.21
$\hat{r}_m^j$ [day^{-1}]	0.002	0.001	0.001	0.002	0.005	0.002	0.003	0.001
$\hat{r}_e^j$ [day^{-1}]	0.09	0.14	0.13	0.08	0.12	0.09	0.07	0.19
$\hat{d}_n^j$ [day^{-1}]	0.04	0.07	0.05	0.03	0.01	0.03	0.06	0.01
λ_p^j [day^{-1}]	0.01	0.01	0.01	0.01	0.01	0.01	0.01	0.01
λ_n^j [day^{-1}]	0.002	0.002	0.002	0.002	0.002	0.002	0.002	0.002
λ_m^j [day^{-1}]	0.07	0.07	0.07	0.07	0.07	0.07	0.07	0.07
K_p^j [cells μL^{-1}]	2942	2091	3195	2244	1121	1490	1322	884
K_s^j [cells μL^{-1}]	2518	1790	2735	1921	960	1275	1131	757
K_m^j [cells μL^{-1}]	27	19	29	21	10	14	12	8
K_e^j [cells μL^{-1}]	2388	1697	2592	1821	910	1209	1073	718
$N^j(t_0)$ [cells μL^{-1}]	1482	618	1360	1281	49	52	111	41
$S^j(t_0)$ [cells μL^{-1}]	106	81	135	164	2	1	10	1
$M^j(t_0)$ [cells μL^{-1}]	309	415	482	1217	7	7	11	8.0
$E^j(t_0)$ [cells μL^{-1}]	1045	975	1217	634	11	11	48	9

Table 5: Population parameter estimates for the fits of the model in **equation S14** (lowest AIC in **Table S2**) to the T cell and virus dynamics. RSE: relative standard error. Empty fields represent cases when the standard deviation of random effects, σ_ψ , was fixed to zero. Values of the fixed effects ($\bar{\psi}$) obtained for $K_p, N\left(t_0\right), R\left(t_0\right), M\left(t_0\right)$, and $E\left(t_0\right)$ had units of absolute cell counts in the model. The values shown here (and used when fitting to data) are in logarithmic scale due to the definition of ψ_j but were transformed after dividing to $5 \times 10^5 \mu$L, the assumed blood volume in a pigtailed macaque (the blood volume was calculated in the same way for all animals, assuming a blood:weight ratio of 100mL/Kg, and body weight of 5Kg). Red values represent a RSE greater than 100%, implying that the number of data points may not be enough to estimate those parameters.

Parameter	ψ	σ_ψ	% **RSE for:**	
			ψ	σ_ψ
$\hat{r}_p$	0.04		21	
$\hat{r}_s$	0.14	0.30	16	29
$\hat{r}_m$	0.003	0.98	458	29
$\hat{r}_e$	0.09	0.33	17	34
$\hat{d}_n$	1.4	1.02	64	37
λ_p	0.01		24	
λ_n	0.004		26	
λ_m	0.09		29	
K_p	3.2	0.17	1	25
K_s	0.10		26	
K_m	1.5		126	
K_e	0.12		24	
$N\left(t_0\right)$	1.7	0.14	1	46
$R\left(t_0\right)$	0.35	0.39	4	43
$M\left(t_0\right)$	0.89	0.12	2	186
$E\left(t_0\right)$	1.2	0.31	3	43
β	-3.5	0.61	6	26
ω_4	-1.2	0.43	5	28
ω_8	-2.4	0.53	5	33
d_h	0.05		21	
I_{50}	-0.69		7	
Δ_t	7.5	0.50	20	31
σ_N	0.19		5	
σ_R	0.12		5	
σ_C	0.16		5	
σ_E	0.19		10	
σ_M	0.25		10	
σ_V	0.69		8	

Table 6: Individual parameter estimates for the fits of the model in **equation S14** (lowest AIC in **Table S2**) to the T cell and virus dynamics. Values obtained for $K_p, N(t_0), R(t_0), M(t_0)$, and $E(t_0)$ had units of absolute cell counts in the model. The values shown here were transformed after dividing to $5 \times 10^5 \mu$L, the assumed blood volume in macaques (the blood volume was calculated in the same way for all animals, assuming a blood:weight ratio of 100mL/Kg, and body weight of 5Kg). Initial values for the control group where obtained from **equation S13**.

	Control				**Transplant**			
	Z09087	**Z09106**	**Z09192**	**Z09204**	**Z09144**	**Z08214**	**A11200**	**Z09196**
$\hat{r}_p^j$ [day^{-1}]	0.04	0.04	0.04	0.04	0.04	0.04	0.04	0.04
$\hat{r}_s^j$ [day^{-1}]	0.21	0.12	0.16	0.12	0.12	0.16	0.08	0.19
$\hat{r}_m^j$ [day^{-1}]	0.002	0.001	0.001	0.003	0.014	0.004	0.007	0.002
$\hat{r}_e^j$ [day^{-1}]	0.08	0.10	0.11	0.07	0.10	0.09	0.07	0.17
$\hat{d}_n^j$ [day^{-1}]	0.01	0.02	0.01	0.01	0.01	0.01	0.03	0.01
λ_p^j [day^{-1}]	0.01	0.01	0.01	0.01	0.01	0.01	0.01	0.01
λ_n^j [day^{-1}]	0.004	0.004	0.004	0.004	0.004	0.004	0.004	0.004
λ_m^j [day^{-1}]	0.09	0.09	0.09	0.09	0.09	0.09	0.09	0.09
K_p^j [cells μL^{-1}]	2571	1957	3032	2201	1125	1398	1057	1056
K_s^j [cells μL^{-1}]	2054	1564	2423	1759	899	1117	844	844
K_m^j [cells μL^{-1}]	76	58	90	65	33	41	31	31
K_e^j [cells μL^{-1}]	1945	1480	2294	1665	851	1057	799	799
$N^j(t_0)$ [cells μL^{-1}]	1311	558	1254	1244	43	38	74	38
$S^j(t_0)$ [cells μL^{-1}]	104	75	126	167	2	1	9	1
$M^j(t_0)$ [cells μL^{-1}]	257	353	458	151	7.0	7.3	9.2	7.4
$E^j(t_0)$ [cells μL^{-1}]	896	973	1194	637	13	12	50	11
β [μL copies^{-1} day^{-1}]	0.0009	0.0003	0.0002	0.0001	0.0002	0.0057	0.0001	0.0002
ω_4 [μL cells^{-1} day^{-1}]	0.08	0.05	0.02	0.04	0.19	0.38	0.06	0.03
ω_8 [μL cells^{-1} day^{-1}]	0.013	0.006	0.003	0.029	0.002	0.001	0.006	0.002
d_h [day^{-1}]	0.05	0.05	0.05	0.05	0.05	0.05	0.05	0.05
I_{50} [cells μL^{-1}]	0.20	0.20	0.20	0.20	0.20	0.20	0.20	0.20
Δ_t [days]	5.9	4.5	6.4	6.7	7.3	20.1	10.4	7.6

7 Supplementary References

1. Lavielle M. Mixed Effects Models for the Population Approach: Models, Tasks, Methods and Tools (ed 1 edition). Boca Raton: Chapman and Hall/CRC; 2014.

2. Burnham KP, Anderson DR. Model Selection and Multimodel Inference: A Practical Information-Theoretic Approach (ed 2). New York: Springer-Verlag; 2002.

3. Schluns KS, Williams K, Ma A, Zheng XX, Lefrancois L. Cutting Edge: Requirement for IL-15 in the Generation of Primary and Memory Antigen-Specific CD8 T Cells. *The Journal of Immunology*. 2002;168(10):4827-4831.

4. Schluns KS, Kieper WC, Jameson SC, Lefrancois L. Interleukin-7 mediates the homeostasis of naïve and memory CD8 T cells *in vivo*. *Nature Immunology*. 2000;1(5):426-432.